High-Performance Coils and Yarns of Polymeric Piezoelectric Nanofibers

Mahmoud Baniasadi,[†] Jiacheng Huang,[†] Zhe Xu,[†] Salvador Moreno,[†] Xi Yang,[‡] Jason Chang,[§] Manuel Angel Quevedo-Lopez,[‡] Mohammad Naraghi,[⊥] and Majid Minary-Jolandan*,[†,∥]

[†]Department of Mechanical Engineering, [‡]Department of Materials Science and Engineering, [§]Department of Bioengineering, [∥]UT Dallas NanoTech Institute, University of Texas at Dallas, 800 W. Campbell Rd., Richardson, Texas 75080, United States
[⊥]Department of Aerospace Engineering, Texas A&M University, 3141 TAMU, College Station, Texas 77843-3141, United States

Ⓢ Supporting Information

ABSTRACT: We report on highly stretchable piezoelectric structures of electrospun PVDF-TrFE nanofibers. We fabricated nanofibrous PVDF-TrFE yarns via twisting their electrospun ribbons. Our results show that the twisting process not only increases the failure strain but also increases overall strength and toughness. The nanofibrous yarns achieved a remarkable energy to failure of up to 98 J/g. Through overtwisting process, we fabricated polymeric coils out of twisted yarns that stretched up to ∼740% strain. This enhancement in mechanical properties is likely induced by increased interactions between nanofibers, contributed by friction and van der Waals interactions, as well as favorable surface charge (Columbic) interactions as a result of piezoelectric effect, for which we present a theoretical model. The fabricated yarns and coils show great promise for applications in high-performance lightweight structural materials and superstretchable piezoelectric devices and flexible energy harvesting applications.

KEYWORDS: piezoelectricity, multifunctional materials, electrospun PVDF nanofibers, mechanical properties, stretchable materials

■ INTRODUCTION

Development of lightweight, strong, and tough materials is critical for current advanced applications such as defense, automobile, and aerospace. Fibrous materials such as nano-fibers, nanotubes, and their twisted yarns are great candidates to achieve this multifunctionality facilitated by their lightweight and enhanced interaction surface.[1−9] Current research is focused on improving the interfacial properties between individual elements in twisted yarns, given that interfaces are often the weakest points in the structure. The weak shear interaction between adjacent nanofibers or nanotubes prevents these materials from achieving their maximum theoretical performance. Interaction between neighboring elements in fibrous materials is often weak van der Waals (vdW) forces or hydrogen bonds if they are properly functionalized. There has been major effort in establishing hydrogen bonds at interfaces, including hydrogen bonds in carbon nanotube (CNT) yarns.[9,10] Electrostatic (Columbic) interactions are much stronger than vdW interactions (∼1 kT) and hydrogen bonds (∼10 kT).[11] Columbic interactions can be as strong as covalent bonds (100−300 kT). Engineering interfaces with endogenous electrostatic interactions can be beneficial in enhancing the interface strength and ultimately results in lightweight materials. Such interactions are believed to exist between collagen fibrils in bone. Collagen fibrils are piezoelectric materials and, hence, would generate surface charges in bone under deforma-tion.[12−14] This mechanism could be one of the reasons for high toughness of natural materials such as bone.

One potential candidate for engineering interfaces with electrostatic (Columbic) interaction would be piezoelectric materials. Mechanical tension in these materials results in surface charges that could enhance the mechanics of the interface. Piezoelectric materials are an important class of multifunctional materials;[15] extensively used as actuators and sensors[16] and in energy harvesting.[17] Common piezoelectric materials such as PZT (lead zirconate titanate), $BaTiO_3$ (barium-titanate), ZnO (zinc oxide), and GaN (gallium nitride), which are often ceramics or semiconductors, are mechanically brittle and fail at low strains (<0.1−3%).[18,19] In contrast to the inherent brittleness of piezoelectric ceramics, piezoelectric polymers have demonstrated a great potential to achieve flexibility and stretchability. Among piezoelectric polymers, the piezoelectric properties of polyvinylidene fluoride (PVDF),[20] and its copolymer PVDF-TrFE (polyvinylidene fluoride trifluoroethylene) has attracted considerable inter-est.[18,21−25] Bulk PVDF has a failure strain in the range of 12−50%.[26,27] In addition, PVDF is biocompatible and is considered a highly attractive polymer for biomedical applications such as in smart catheter devices and as scaffold for tissue engineer-ing.[28−30]

PVDF is semicrystalline and approximately 50% amorphous with several stable crystalline forms including α, β, γ, and δ
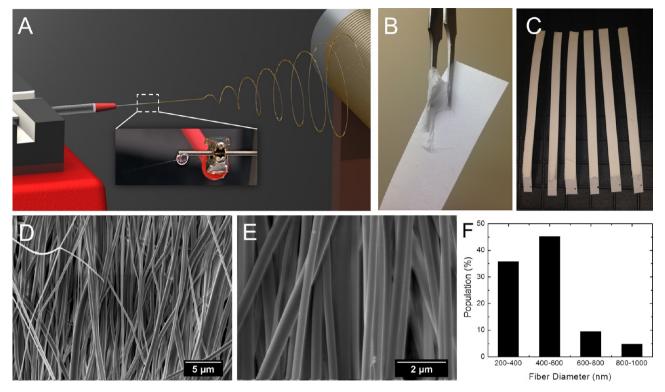
Figure 1. (A) Schematic of the electrospinning process; (inset) jet of PVDF-TrFE solution projected from the tip of the needle toward the collector. (B) Electrospun membrane detached from the substrate using tweezers and (C) cut into ribbons. (D and E) SEM micrographs of a ribbon (membrane) with aligned nanofibers. (F) Histogram of the distribution of the fibers diameters obtained from SEM images. More than 80% of nanofibers have diameters of 200−600 nm.

phases. The β-phase is the most piezoelectrically responsive one. PVDF is mechanically stretched and electrically poled at very high voltage under elevated temperature (80−150 °C) to align randomly oriented dipoles in the sample.[27] On the basis of recent reports, electrospun PVDF and PVDF-TrFE nanofibers have shown great promise both in terms of structural functionality,[31] as well as energy harvesting and sensor applications.[32−38] It is reported that electrospun nanofibers can sustain mechanical strain up to 65%.[31] Aligned arrays of electrospun PVDF-TrFE nanofibers enabled ultrahigh sensitivity for measuring pressure, even at exceptionally small values (0.1 Pa).[34] Recently, electrospun nanofibers of PVDF were demonstrated for self-powering wearable electronic textiles applications.[33,37,38]

In this study, we report on highly stretchable piezoelectric structures of electrospun PVDF-TrFE nanofibers. We used twisting process to develop nanofibrous PVDF-TrFE yarns out of ribbons. Our results show that the twisting process not only increases the failure strain but also increases overall strength and toughness. Through overtwisting, we fabricated novel polymeric coils out of twisted yarns. Overtwisting here means that once the yarn samples were obtained by twisting the ribbons, we apply additional twist to fabricate coil samples from yarn samples. The coils can stretch up to ∼740% strain. This enhancement in mechanical properties is likely a result of increased interactions between nanofibers, contributed by friction and vdW interactions, as well as favorable surface charge interactions as a result of piezoelectric effect. We present a theoretical model to account for contribution of piezoelectric effect in mechanical properties.

RESULTS AND DISCUSSION

The nanofibrous membrane was separated from the substrate and was cut into several identical sized ribbons, as shown in Figure 1C. Figure 1D,E shows SEM (scanning electron microscope) images of the aligned nanofibrous membranes. More than 80% of the nanofibers have a diameter of 200−600 nm (Figure 1F).

Figure 2 shows the FTIR and XRD spectra acquired from the samples. The FTIR peak at 840 cm^{-1} is the main peak associated with the β-phase.[39,40] In FTIR spectra, α-phase would be represented with peaks at 765 and 795 cm^{-1}. Absence of strong peaks at this wavenumbers indicates that the β-phase is the majority phase in these samples. X-ray diffraction (XRD) data is shown in Figure 2D,E. The strong peak at $2\theta \sim 19°−20°$ corresponds to XRD from (110) plane, representing the β-phase, which confirms the presence of the β-phase in the nanofibers. Presence of strong β-phase in the electrospun nanofibers shows that electrospun PVDF-TrFE gets poled during electrospinning, and the commonly used stretching at an elevated temperature is not necessary to obtain β-phase. The importance of β-phase is that the nanofibers are piezoelectric, as shown next.

The presence of β-phase in the nanofibers points to strong piezoelectric properties. For quantitative analysis, we characterized piezoelectric properties of PVDF-TrFE nanofibers using both direct and converse methods (Figure 3).[15,16] In the direct method, electric charge generated in the sample under mechanical deformation was measured. In the converse method, we measured displacement generated under electrical voltage. For direct measurement, we used a flexure stage that subjected PVDF-TrFE nanofibers to a periodic flexed-unflexed configuration. As shown in Figure 3A, the sample is mounted
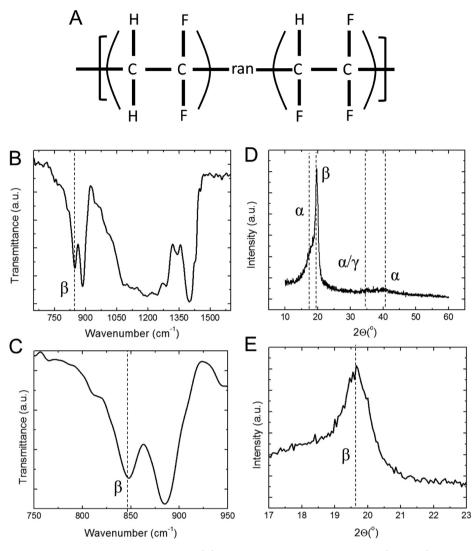
Figure 2. FTIR and XRD spectra of the electrospun nanofibers: (A) Chemical structure of PVDF-TrFE. (B and C) FTIR spectra showing the peak associated with the crystalline β-phase. (D and E) XRD spectra showing the peak at $2\theta = 19° \sim 20°$ that corresponds to the X-ray diffraction pattern from (110) plane, representing the β-phase.
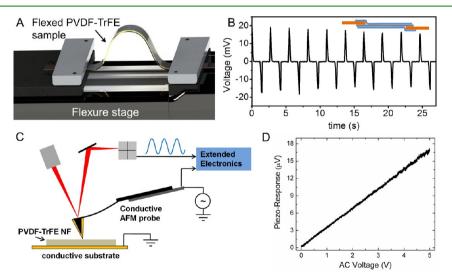

Figure 3. Piezoelectric characterization of the electrospun nanofibers: (A) Schematic of the flexure-test experiment. (B) Plot shows the generated voltage for several flexed and unflexed states; (inset) schematic of the prepared sample. (C) Schematic of the PFM experiment. (D) Piezoresponse amplitude vs applied voltage from PVDF-TrFE nanofiber.

on the flexure stage, and the electrodes of the sample are connected to a multimeter. The experimental setup is shown in Figure S1 (Supporting Information). The generated voltage from the sample is shown in Figure 3B. Each stroke of the flexure stage results in two peaks in opposite directions. The first peak is the result of flexing deformation, and the second peak is the result of unflexing (relaxing) deformation (Figure S1B,C, Supporting Information). The nanofibers generate a uniform voltage as large as 20 mV. By improving the electrical contact through fabricating the nanofiber layer along with incorporating the electrodes within the structure of the device, we can obtained improved electrical output.[33]

For converse piezoelectric characterization, we used piezoresponse force microscopy (PFM), Figure 3C.[12,16] Figure 3D shows the obtained response on an individual nanofiber. The relationship between the applied voltage and measured piezo-response is linear, which indicates that the measured response is the piezoelectric response. The piezoelectric constant of the nanofiber was measured to be 37−48 pm/V, which is slightly stronger than the bulk PVDF-TrFE (∼38 pm/V). This indicates that the fabricated nanofibers from electrospinning are highly piezoelectric without the need to the electric poling, which confirms the results of FTIR and XRD for the presence of β-phase in the nanofibers.

Yarns and coils were fabricated by twisting the ribbons,[7,41,42] as shown in Figure 4. Detail of the experimental method is
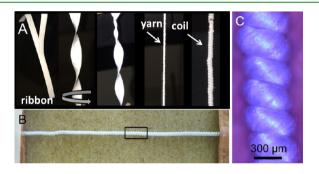

Figure 4. (A) Fabrication of yarns and coils from electrospun ribbons by twisting process. (B) A coil several centimeters long. (C) Optical microscope image of a coil.

shown in Figure S4 (Supporting Information). During the twisting process, a small weight was hanged from one end of the ribbon, while the other end of the sample was fixed. The end of the ribbon was twisted using a DC motor. After application of twists to a ribbon, initially a uniform yarn was obtained. When the yarn was overtwisted, coils started developing from one end of the yarn, and gradually extended to the other end of the sample until the entire yarn was converted to a fully packed coil. For each sample, number of turns was counted during twisting process. This number was divided by length of the sample to provide an "index" for the number of turns per length of the sample. These values are provided in Table S1 (Supporting Information). Figure 4B,C shows images of the fabricated coils. Yarns and coils several centimeter long can be fabricated using this method.

Figure 5 shows SEM micrographs of coil and yarn samples fabricated from aligned nanofibers. The coil has an outer diameter of ∼306 μm and a pitch of 140 μm. SEM images shows that the coil is uniform along its length. In addition, the high-magnification images show that alignment of the nanofibers is maintained in the fabricated coil after twisting and

overtwisting process. Figure 5J−L show SEM micrographs of a yarn with a diameter of 175 μm. Similar to the coil, the yarn is made of aligned nanofibers. Figures S5−S7 (Supporting Information) show SEM images of more coil and yarn samples with random and aligned nanofibers.

An important observation from SEM images is that even after a large amount of twisting, the nanofibers in the fabricated samples appear to be continuous with no signs of nanofiber failure. This shows that individual nanofibers are highly deformable. The stretchability and continuous geometry of the nanofibers would contribute to the enhanced mechanical properties of the samples. To examine the mechanical properties of the samples, the fabricated ribbons, yarns, and coils were subjected to uniaxial tensile test. Results of the tensile experiments of the ribbons and yarns fabricated from aligned nanofibers are shown in Figure 6. Figure S8 (Supporting Information) shows the corresponding results for the samples fabricated from random nanofibers. Table S1 (Supporting Information) presents the detailed mechanical properties of the samples.

The results of the tensile experiment are given in terms of the specific stress vs engineering strain. The engineering strain was calculated as the crosshead displacement divided by the gauge length of the sample, $\varepsilon = ((L - L_0)/L_0) = (\Delta L/L_0)$. The specific stress of the sample was calculated by dividing the force sustained by the sample by the linear density (λ) of the sample. The linear density is defined as

$$\lambda = \frac{\text{weight (g)}}{\text{length (km)}} \tag{1}$$

where λ is defined in "tex" units. In these units, the specific stress has units of N/g/km, which is equivalent to 10^3 MPa/g/cm^3. Density of PVDF-TrFE is 1.87 g/cm^3. Area under force−extension was calculated for each sample and normalized by weight to provide gravimetric toughness in units of J/g.

Inset in Figure 6A shows digital photographs of a ribbon sample under tension. Aligned ribbons show strain to failure in the range of 67−83%. Comparing to Figure S8A (Supporting Information), ribbons made of random nanofibers show 134−146% failure strain, on average more than 1.8 times larger than the aligned ribbons. However, the strength of the aligned ribbons is on average 8.7 times larger than the random ribbons. The toughness of the aligned ribbons is also more than five times larger than the random samples. The higher ductility of ribbons with randomly oriented nanofibers is likely the result of additional degrees of motion available to misaligned nanofibers, such as reorientation toward the loading direction. This reorientation is, however, accompanied by nonuniform stress distribution and localization, compromising the overall strength and toughness.

Similar trends hold for the yarn samples. The strain to failure of the random samples is larger (by a factor of 1.6) compared to the aligned yarns. However, their toughness and strength are larger compared to the random yarns by factors of 6 and 9, respectively. The yarns fabricated from the random samples stretch up to 235% strain, while for the aligned samples, the strain to failure reduces to ∼160%.

The aligned yarns of PVDF-TrFE achieve a remarkable energy to failure of up to 98 J/g. This is notable considering that a large portion of previous fibers such as CNT yarns or high-performance synthetic fibers (e.g., Kevlar) show energy to failure in the range of 30−60 J/g. For instance, the energy-to-
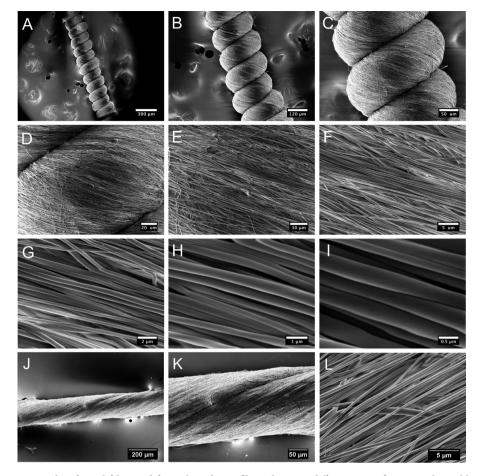
Figure 5. (A−I) SEM micrographs of a coil fabricated from aligned nanofibers shown in different magnifications. The coil has an outer diameter of ∼306 μm and a pitch of 140 μm. (J−L) SEM micrographs of a yarn fabricated from aligned nanofibers shown in different magnifications. The yarn has a diameter of ∼175 μm.
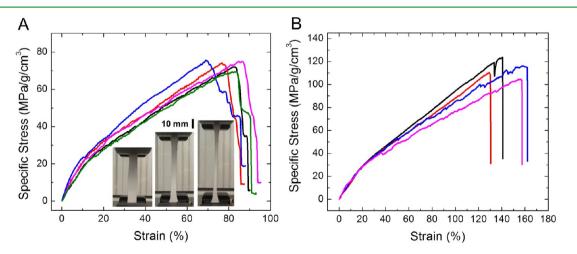

Figure 6. Tensile experiment results in terms of specific stress vs strain for (A) ribbons and (B) yarns. (A, inset) digital photographs of the tensile experiment on a ribbon.

failure of CNT yarns were fabricated by pulling CNT aerogels from a chemical vapor deposition (CVD) reactor and twisting them into yarns, or via hot-drawing polymer−CNT composite fibers, and CNT yarns drawn from CNT forests are typically within 14−60 J/g.[2,43,44] This is considerably lower than the highest energy-to-failure of PVDF-TrFE yarns reported here. On the other hand, in few cases, CNT yarns have been developed with energy-to-failures of ∼100 J/g or higher,[10] comparable to values reported here for PVDF yarns.

Yarn samples show higher performance compared to the ribbon samples in terms of failure strain, strength and toughness. This enhancement of mechanical properties is the result of increased nanofiber−nanofiber interactions in the yarns, facilitated by the lower porosity (more compactness) of the yarns as the result of twisting process. The nature of

interactions between nanofibers is likely vdW (van der Waals) interactions, and sliding friction. In addition, nanofibers become poled during the electrospinning process as confirmed by FTIR and X-ray spectroscopy (Figure 2) and direct piezoelectric characterization (Figure 3). Therefore, the interactions between nanofibers can also originate from favorable (attractive) electrostatic interactions of neighboring nanofibers. This electrostatic interaction is shown in Figure 7. These electro-
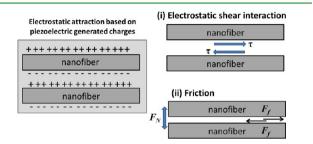

Figure 7. (Left) Electrostatic interactions between adjacent piezoelectric nanofibers as the result of piezoelectric generated surface charges under mechanical stress. (i) Contribution of electrostatic surface charges to shear force between nanofibers. (ii) Contribution of electrostatic forces to the friction between nanofibers by increasing the normal compressive force between the nanofibers.

static surface charges are generated as the result of piezoelectric effect when the nanofibers are under mechanical stress. As a result, this electrostatic interaction may enhance the mechanical properties of the yarn samples, given that electrostatic interactions are much stronger than weak vdW forces.[11] For

the nanofiber sample in a yarn, it can be shown that (Supporting Information)

$$\frac{U_e}{U_{\text{Elastic}}} = \frac{E d_{13}^2}{\varepsilon_0} \times \frac{1 - v_F}{v_F} \qquad (2)$$

where U_e and U_{Elastic} are the elastic energy in the nanofibers and the electrostatic energy stored between the nanofibers, respectively. E, d_{13}, and ε_0 are the elastic modulus, the piezoelectric constant of PVDF-TrFE, and the permittivity of the air, respectively, and v_F is the volume fraction of the nanofibers. Volume fraction of the nanofibers can be estimated from the porosity of the samples. For example, for yarn samples, the volume fraction of nanofibers is ~40% (Supporting Information). For PVDF-TrFE yarns, the (U_e/U_{Elastic}) is ~2.07, meaning that the electrostatic energy can be comparable to or even larger than the elastic energy stored in the nanofibers. This effect is likely less in ribbons, given the smaller number of fiber−fiber interactions, whereas in yarns, the twisting process increases fiber−fiber interactions.

Another contribution of the piezoelectric generated surface charges could arise from enhancing the friction between the nanofibers. This phenomena is often called electrostatic tribocharging.[45,46] It has been suggested that tribocharges produced by friction have a large effect on the friction coefficient of dielectrics and may exceed all other mechanical energy dissipation mechanisms.[46] Friction force is proportional to normal force between two surfaces ($F_f = \mu F_N$). The attractive force between surface charges on the nanofibers will increase the normal force between nanofibers, and hence contribute to
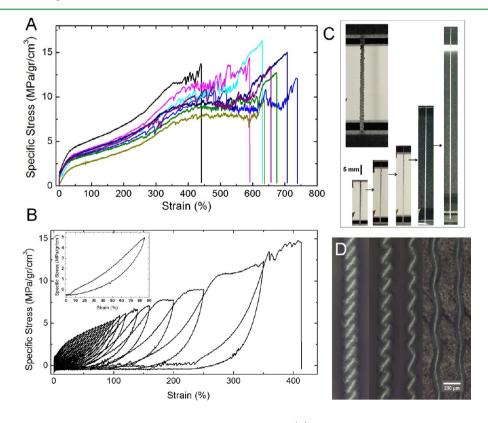

Figure 8. (A) Tensile experiment results in terms of specific stress vs strain for coils. (B) Load-unload response of a coil sample; (inset) load−unload up to 85% strain with full return to zero strain after unloading. (C) Digital photographs of the tensile testing of a PVDF-TrFE coil showing the extension of the coil under tension up to ~700% strain, to the point that all the coils are uncoiled. (D) A series of optical microscope images showing deformation mechanism during the extension of a coil under axial stretch (left to right). The coil becomes straight, resembling a yarn shown in the right panel.
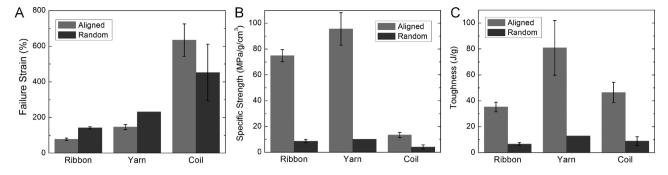
Figure 9. Comparison of mechanical properties of aligned and random ribbons, yarns, and coils: (A) failure strain, (B) specific strength, and (C) toughness.

the static friction between nanofibers. This effect, in turn, will enhance interaction forces between the nanofibers (Figure 7ii.

Figure 8A shows the tensile experiment results for coils made of aligned nanofibers. The coil samples stretch up to remarkable strain of ~740%. For random coils, failure strain range drops to 328−632% strain. Aligned coils also show much larger toughness and strength compared to the random coils. Figure 8B shows a coil sample subjected to a series of load-unload until final failure. The sample shows a hysteretic behavior under loading and unloading cycles; up to ~85% strain (Figure 8B, inset), the strain returns to zero after unloading, indicating elastic behavior. Further strain results in plastic deformation. Figure 8C shows consecutive images of a coil under tension. This coil sustains strain up to nearly 700% before failure. Figure 8D shows a series of optical microscope images from deformation of a coil sample under an optical microscope. The deformation mechanism of the coil is initially separation of the adjacent coils surfaces and gradual unwinding of the coils until the sample is free of coils. Similar CNT coils reported in the literature show strain to failure of ~285%, with a toughness of 28.7 J/g and tensile strength of ~74 MPa.[8] The PVDF-TrFE coil samples reported here achieved toughness of up to 56 J/g and a tensile strength of up to 30.5 MPa.

Figure 9 shows a summary of the mechanical properties of the random and aligned ribbon, yarn, and coil samples. Coil samples achieve the highest strain to failure, facilitated by the structural geometry. Specific strength of the aligned samples is several folds larger than the random samples. The yarns show the largest enhancement of specific strength by 9.4 times compared to the random yarns. Ribbons and coils exhibit 8.7 and 4.8 times enhancement of specific strength, respectively, compared to the corresponding random samples. This large enhancement in specific strength can be explained by increased number of nanofibers that contribute to load carrying in the axial direction of the sample. Yarns achieve the highest toughness in comparison to ribbon and coils. Compared to ribbons, yarn and coil samples have larger fiber−fiber interactions as the result of twisting process. Moreover, according to SEM images, the interaction length of adjacent nanofibers in yarns is longer than coils. This is due to the overtwisting process in coils, which reduces the interaction length by rotating the nanofibers along the pitch of the coil. The increased interaction length in yarns facilitates the load transfer between nanofibers, caused by a combination of vdW interactions, favorable electrostatic interactions, and piezo-electrically enhanced friction, leading to enhanced toughness and strength.

CONCLUSIONS

We demonstrated that highly stretchable yarns and coils can be fabricated by taking advantage of the twisting process of electrospun piezoelectric PVDF-TrFE nanofibers. Superstretch-able coils exhibited strain to failure of up to 740%. The nanofibrous yarns achieve a remarkable energy to failure up to 98 J/g. The optimal twisting condition for yarns, which is in between untwisted ribbons and overtwisted coils, increases the interaction length between nanofibers in yarns. The increased interaction length facilitates load-transfer between nanofibers, through a combination of vdW interactions, favorable columbic interactions, and piezoelectrically enhanced friction, leading to enhanced toughness and strength.

EXPERIMENTAL SECTION

Electrospinning Process. We used electrospinning process to fabricate PVDF-TrFE nanofibers, Figure 1A. The nanofibers were collected on a rotating drum collector. By changing the rotational speed of the collector drum, we obtained random and aligned nanofibers. The rotational speed of the collector drum was 120 and 4300 rpm for random and aligned nanofibers, respectively. Dimethylformamide (DMF, Sigma-Aldrich) was used as the solvent for PVDF-TrFE powder. The final solution contained 20% PVDF-TrFE. The solvent contained 30% DMF and 70% acetone. The diameter of the needle in the electrospinning setup was 1 mm. A dc electric voltage of 25 kV was applied between the needle tip and the collector placed at a distance of 25 cm.

FTIR Spectroscopy and XRD. A PerkinElmer GX FTIR spectrometer was used for collecting the IR spectra from the samples. X-ray diffraction of samples was recorded using a Rigaku Ultima III XRD (40 kV, Rigaku Corp., Tokyo, Japan) with Cu $K\alpha$ source (wavelength, 0.15418 nm). The diffractogram was recorded between angles 2θ = 10 and 60° with a scan rate of 3° per minute at room temperature.

Tensile Experiments. Mechanical properties of the samples were characterized using uniaxial tension (Instron Universal testing machine 5969). Each end of the sample was glued onto a flat grip using epoxy glue. Samples were subjected to displacement rate of 1.2 mm/s. This rate was chosen as a quasi-static strain rate for the experiments. Effect of higher or lower rates was not studied in this work. Before the experiment, we obtained the gauge length (L_0) of each sample using a digital caliper.

Piezoelectric Characterization. For flexure experiments (Figure S1, Supporting Information), samples were fabricated as following. A PVDF-TrFE ribbon was sandwiched between two aluminum foils and was subsequently mounted between two Kapton tapes (50 μm thickness). Double-sided copper tape was used as the electrode. The electrodes were mounted between grippers of a flexure stage (SIGMA KOKI Co., Japan). The electrodes were connected to a digital multimeter (Agilent 34410A). A customized LabView interface was developed to simultaneously run the flexure stage controller and record the generated voltage from the multimeter.

PFM experiments were conducted using a MFP-3D Asylum atomic force microscope (AFM). Conductive AFM cantilevers with a spring constant of ~5 N/m and a resonance frequency of ~160 kHz were used. PVDF-TrFE nanofibers were directly electrospun onto a gold-coated Si substrate (Figure S2, Supporting Information). An ac electric potential ($A \sin (\omega t)$) was applied between the AFM probe as the top electrode and the gold-coated substrate as the bottom electrode, where A is the amplitude and ω is the frequency of the applied electric field. A frequency sweep was conducted to identify the resonance peak of the tip–sample at contact. PFM ramp experiments were conducted at 100 kHz, away from the tip–sample resonance. PFM ramp experiments consisted of applying a voltage sweep up to 5 V on the nanofiber. To calibrate the sensitivity of the PFM experiments, a periodically poled lithium niobate calibration standard was used. The d_{33} piezoelectric constant of the poled lithium niobate is 21–27 pm/V.

■ ASSOCIATED CONTENT

Ⓢ Supporting Information

Setup for characterization of piezoelectric properties, optical microscope image of PVDF-TrFE nanofibers, additional SEM and optical microscope images of the fabricated yarns and coils, mechanical properties of random nanofiber samples, table of mechanical properties, and detail derivation of the theoretical model. This material is available free of charge via the Internet at http://pubs.acs.org.

■ AUTHOR INFORMATION

Corresponding Author
*E-mail: majid.minary@utdallas.edu.

Notes
The authors declare no competing financial interest.

■ ACKNOWLEDGMENTS

■ REFERENCES

(1) Qian, D.; Wagner, G. J.; Liu, W. K.; Yu, M. F.; Ruoff, R. S. Mechanics of Carbon Nanotubes. *Appl. Mech. Rev.* **2002**, *55*, 495–533.

(2) Zhang, M.; Atkinson, K. R.; Baughman, R. H. Multifunctional Carbon Nanotube Yarns by Downsizing an Ancient Technology. *Science* **2004**, *306*, 1358–1361.

(3) Lima, M. D.; Fang, S.; Lepró, X.; Lewis, C.; Ovalle-Robles, R.; Carretero-González, J.; Castillo-Martínez, E.; Kozlov, M. E.; Oh, J.; Rawat, N.; Haines, C. S.; Haque, M. H.; Aare, V.; Stoughton, S.; Zakhidov, A. A.; Baughman, R. H. Biscrolling Nanotube Sheets and Functional Guests into Yarns. *Science* **2011**, *331*, 51–55.

(4) Naraghi, M.; Filleter, T.; Moravsky, A.; Locascio, M.; Loutfy, R. O.; Espinosa, H. D. A Multiscale Study of High Performance Double-Walled Nanotube-Polymer Fibers. *ACS Nano* **2010**, *4*, 6463–6476.

(5) Shin, M. K.; Lee, B.; Kim, S. H.; Lee, J. A.; Spinks, G. M.; Gambhir, S.; Wallace, G. G.; Kozlov, M. E.; Baughman, R. H.; Kim, S. J. Synergistic Toughening of Composite Fibres by Self-Alignment of Reduced Graphene Oxide and Carbon Nanotubes. *Nat. Commun.* **2012**, *3*, 650.

(6) Motta, M.; Li; Kinloch, I.; Windle, A. Mechanical Properties of Continuously Spun Fibers of Carbon Nanotubes. *Nano Lett.* **2005**, *5*, 1529–1533.

(7) Jiang, K. L.; Li, Q. Q.; Fan, S. S. Nanotechnology: Spinning Continuous Carbon Nanotube Yarns. Carbon Nanotubes Weave Their Way into a Range of Imaginative Macroscopic Applications. *Nature* **2002**, *419*, 801–801.

(8) Shang, Y.; He, X.; Li, Y.; Zhang, L.; Li, Z.; Ji, C.; Shi, E.; Li, P.; Zhu, K.; Peng, Q.; Wang, C.; Zhang, X.; Wang, R.; Wei, J.; Wang, K.; Zhu, H.; Wu, D.; Cao, A. Super-Stretchable Spring-Like Carbon Nanotube Ropes. *Adv. Mater.* **2012**, *24*, 2896–2900.

(9) Beese, A. M.; Sarkar, S.; Nair, A.; Naraghi, M.; An, Z.; Moravsky, A.; Loutfy, R. O.; Buehler, M. J.; Nguyen, S. T.; Espinosa, H. D. Bio-Inspired Carbon Nanotube-Polymer Composite Yarns with Hydrogen Bond-Mediated Lateral Interactions. *ACS Nano* **2013**, *7*, 3434–3446.

(10) Naraghi, M.; Filleter, T.; Moravsky, A.; Locascio, M.; Loutfy, R. O.; Espinosa, H. D. A Multiscale Study of High Performance Double-Walled Nanotube−Polymer Fibers. *ACS Nano* **2010**, *4*, 6463–6476.

(11) Israelachvili, J. N. *Intermolecular and Surface Forces*. Academic Press: Burlington, MA, 2011.

(12) Minary-Jolandan, M.; Yu, M.-F. Nanoscale Characterization of Isolated Individual Type I Collagen Fibrils: Polarization and Piezoelectricity. *Nanotechnology* **2009**, *20*, 085706.

(13) Minary-Jolandan, M.; Yu, M.-F. Uncovering Nanoscale Electromechanical Heterogeneity in the Subfibrillar Structure of Collagen Fibrils Responsible for the Piezoelectricity of Bone. *ACS Nano* **2009**, *3*, 1859–1863.

(14) Minary-Jolandan, M.; Yu, M. F. Shear Piezoelectricity in Bone at the Nanoscale. *Appl. Phys. Lett.*, **2010**, *97*.

(15) Minary-Jolandan, M.; Yu, M.-F. Mechanical and Electromechanical Characterization of One-Dimensional Piezoelectric Nanomaterials. In *Piezoelectric Nanomaterials for Biomedical Applications*; Ciofani, G.; Menciassi, A., Eds. Springer 2012.

(16) Espinosa, H. D.; Bernal, R. A.; Minary-Jolandan, M. A Review of Mechanical and Electromechanical Properties of Piezoelectric Nanowires. *Adv. Mater.* **2012**, *24*, 4656–4675.

(17) Rome, L. C.; Flynn, L.; Goldman, E. M.; Yoo, T. D. Generating Electricity While Walking with Loads. *Science* **2005**, *309*, 1725–1728.

(18) Lingam, D.; Parikh, A. R.; Huang, J.; Jain, A.; Minary-Jolandan, M. Nano/Microscale Pyroelectric Energy Harvesting: Challenges and Opportunities. *Int. J. Smart Nano Mater.* **2013**, 1–17.

(19) Bernal, R. A.; Agrawal, R.; Peng, B.; Bertness, K. A.; Sanford, N. A.; Davydov, A. V.; Espinosa, H. D. Effect of Growth Orientation and Diameter on the Elasticity of GaN Nanowires. A Combined in Situ TEM and Atomistic Modeling Investigation. *Nano Lett.* **2010**, *11*, 548–555.

(20) Kawai, H. The Piezoelectricity in Poly(vinylidene fluoride). *Jpn. J. of Appl. Phys.* **1969**, *8*, 975–976.

(21) Lee, M.; Chen, C. Y.; Wang, S.; Cha, S. N.; Park, Y. J.; Kim, J. M.; Chou, L. J.; Wang, Z. L. A Hybrid Piezoelectric Structure for Wearable Nanogenerators. *Adv. Mater.* **2012**, *24*, 1759–1764.

(22) Vatansever, D.; Hadimani, R. L.; Shah, T.; Siores, E., Voltage Response of Piezoelectric PVDF Films in Vacuum and at Elevated Temperatures. *Smart Mater. Struct.*, **2012**, *21*.

(23) Shenck, N. S.; Paradiso, J. A. Energy Scavenging with Shoe-Mounted Piezoelectrics. *Micro, IEEE* **2001**, *21*, 30–42.

(24) Granstrom, J.; Feenstra, J.; Sodano, H. A.; Farinholt, K. Energy Harvesting from a Backpack Instrumented with Piezoelectric Shoulder Straps. *Smart Mater. Struct.* **2007**, *16*, 1810–1820.

(25) Vatansever, D.; Hadimani, R. L.; Shah, T.; Siores, E., An Investigation of Energy Harvesting from Renewable Sources with PVDF and PZT. *Smart Mater. Struct.*, **2011**, *20*.

(26) SIMONA PVDF Product Information. http://Www.Simona.De/Static/Sites/Default/De/Assets/Informationsmaterial/Englisch/Pi_E/Pvdf_E.Pdf.

(27) Hadimani, R. L.; Bayramol, D. V.; Sion, N.; Shah, T.; Limin, Q.; Shaoxin, S.; Siores, E. Continuous Production of Piezoelectric Pvdf Fibre for E-Textile Applications. *Smart Mater. Struct.* **2013**, *22*, 075017.

(28) Ratner, B. D.; Hoffman, A. S.; Schoen, F. J.; Lemons, J. E. *Biomaterials Science: An Introduction to Materials in Medicine*. Academic Press: Oxford, 2013.

(29) Low, Y. K. A.; Meenubharathi, N.; Niphadkar, N. D.; Boey, F. Y. C.; Ng, K. W. A- and B-Poly(vinylidene fluoride) Evoke Different Cellular Behaviours. *J. Biomater. Sci., Polym. Ed.* **2011**, *22*, 1651–1667.

(30) Sharma, T.; Aroom, K.; Naik, S.; Gill, B.; Zhang, J. X. J. Flexible Thin-Film Pvdf-Trfe Based Pressure Sensor for Smart Catheter Applications. *Ann. Biomed. Eng.* **2013**, *41*, 744−751.

(31) Baji, A.; Mai, Y. W.; Du, X. S.; Wong, S. C. Improved Tensile Strength and Ferroelectric Phase Content of Self-Assembled Polyvinylidene Fluoride Fiber Yarns. *Macromol. Mater. Eng.* **2012**, *297*, 209−213.

(32) Gheibi, A.; Bagherzadeh, R.; Merati, A.; Latifi, M. Electrical Power Generation from Piezoelectric Electrospun Nanofibers Membranes: Electrospinning Parameters Optimization and Effect of Membranes Thickness on Output Electrical Voltage. *J. Polym. Res.* **2014**, *21*, 1−14.

(33) Gheibi, A.; Latifi, M.; Merati, A.; Bagherzadeh, R. Piezoelectric Electrospun Nanofibrous Materials for Self-Powering Wearable Electronic Textiles Applications. *J. Polym. Res.* **2014**, *21*, 1−7.

(34) Persano, L.; Dagdeviren, C.; Su, Y. W.; Zhang, Y. H.; Girardo, S.; Pisignano, D.; Huang, Y. G.; Rogers, J. A., High Performance Piezoelectric Devices Based on Aligned Arrays of Nanofibers of Poly(vinylidenefluoride-co-trifluoroethylene).*Nat. Commun.*,**2013**, *4*.

(35) Chang, C. E.; Tran, V. H.; Wang, J. B.; Fuh, Y. K.; Lin, L. W. Direct-Write Piezoelectric Polymeric Nanogenerator with High Energy Conversion Efficiency. *Nano Lett.* **2010**, *10*, 726−731.

(36) Chang, J.; D, M.; Chang, C.; Lin, L. Piezoelectric Nanofibers for Energy Scavenging Applications. *Nano Energy* **2012**, *1*, 356−371.

(37) Fang, J.; Wang, X.; Lin, T. Electrical Power Generator from Randomly Oriented Electrospun Poly(vinylidene fluoride) Nanofibre Membranes. *J. Mater. Chem.* **2011**, *21*, 11088−11091.

(38) Fang, J.; Wang, X. G.; Lin, T. Power Generation from Randomly Oriented Electrospun Nanofiber Membranes. *Adv. Mater. Res.* **2012**, *340*, 479−481.

(39) Salimi, A.; Yousefi, A. A. Analysis Method: FTIR Studies of B-Phase Crystal Formation in Stretched PVDF Films. *Polym. Test.* **2003**, *22*, 699−704.

(40) Bormashenko, Y.; Pogreb, R.; Stanevsky, O.; Bormashenko, E. Vibrational Spectrum of Pvdf and Its Interpretation. *Polym. Test.* **2004**, *23*, 791−796.

(41) Dalton, A. B.; Collins, S.; Munoz, E.; Razal, J. M.; Ebron, V. H.; Ferraris, J. P.; Coleman, J. N.; Kim, B. G.; Baughman, R. H. Super-Tough Carbon-Nanotube Fibres-These Extraordinary Composite Fibres Can Be Woven into Electronic Textiles. *Nature* **2003**, *423*, 703−706.

(42) Liu, K.; Sun, Y. H.; Zhou, R. F.; Zhu, H. Y.; Wang, J. P.; Liu, L.; Fan, S. S.; Jiang, K. L., Carbon Nanotube Yarns with High Tensile Strength Made by a Twisting and Shrinking Method.*Nanotechnology*,**2010**, *21*.

(43) Miaudet, P.; Badaire, S.; Maugey, M.; Derré, A.; Pichot, V.; Launois, P.; Poulin, P.; Zakri, C. Hot-Drawing of Single and Multiwall Carbon Nanotube Fibers for High Toughness and Alignment. *Nano Lett.* **2005**, *5*, 2212−2215.

(44) Motta, M.; Moisala, A.; Kinloch, I. A.; Windle, A. H. High Performance Fibres from 'Dog Bone' Carbon Nanotubes. *Adv. Mater.* **2007**, *19*, 3721−3726.

(45) LOEB, L. B. The Basic Mechanisms of Static Electrification. *Science* **1945**, *102*, 573−576.

(46) Burgo, T. A. L.; Silva, C. A.; Balestrin, L. B. S.; Galembeck, F. Friction Coefficient Dependence on Electrostatic Tribocharging. *Sci. Rep.* **2013**, *3*, 2384.